

Reduced-order event-triggered controller for a singularly perturbed system: An active suspension case

ISSN 1751-8644

Received on 26th July 2019

Revised 19th June 2020

Accepted on 17th August 2020

E-First on 14th October 2020

doi: 10.1049/iet-cta.2019.0864

www.ietdl.org

Manisha Bhandari¹ ✉, Deepak Fulwani², B. Bandopadhyay³, Rajeev Gupta¹

¹Department of Electronics, Rajasthan Technical University Kota, Kota 324007, Rajasthan, India

²Electrical Department, Indian Institute of Technology Jodhpur, Jodhpur 342011, India

³Systems and Control Engineering Department, Indian Institute of Technology Mumbai, Mumbai 400076, Maharashtra, India

✉ E-mail: mbhandari@rtu.ac.in

Abstract: For two-time scale systems, singular perturbation theory is often used for designing a controller based only on an approximate model of its slow dynamics, assuming the fast model to be stable. In this context, the authors investigate and implement a stabilising event-triggered feedback law for a networked singularly perturbed system, based only on an approximate model of its slow dynamics. Triggering rule guarantees the stability and the existence of a positive lower bound between two consecutive transmissions. The proposed approach has been validated for a laboratory-scale hardware setup of an active suspension system of a quarter-car model. The presence of fast and slow modes in a vehicle suspension system is utilised to model it as a singularly perturbed system. Experimental results indicate that in spite of the simplified structure of the controller and event-triggered feedback, its performance is comparable to that of the full-state feedback design with continuous feedback with the significant reduction in control execution events.

1 Introduction

Physical systems in which slow and fast dynamics coexist are often modelled as singularly perturbed systems (SPSs) or as two-time scale systems [1]. In SPSs, the feedback control synthesis suffers from the higher dimensionality and ill-conditioning due to the simultaneous existence of slow and fast dynamics [2, 3]. The time-scale control strategies permit the original ill-conditioned system to be decomposed into two reduced-order subsystems in different time scales, known as the slow and the fast (boundary layer) subsystems. Control synthesis for the overall system may be obtained by designing stabilising control laws for these subsystems independently, which ensures the stability of the overall system for both linear time-invariant [4] and classes of non-linear systems [5]. Although this methodology is valid for the continuous and periodic sample data control, for many practical situations, when SPS has a resource-limited communication network in the feedback path, how to develop an appropriate control scheme to maintain the control performance is meaningful.

Event-triggered control (ETC) proposed in recent years has received significant research interest because of its potential application in networked control systems (NCSs) or embedded systems, where computation and communication resources are limited [6, 7]. In this control technique, the control execution does not take place periodically but only when a certain condition on the plant state gets violated [8–13]. Thus, compared to periodic sampling, ETC is more effective in making regulated uses of the network resources [14, 15]. Real-time implementation of ETC system requires that the control update times should not be arbitrarily close. In other words, there can not be infinite triggering instants in a finite time known as Zeno effect [8]. There has been remarkable contribution in the field of ETC in recent years. Authors have studied ETC with output feedback in [16, 17], event-triggered quantisation in [18]. Various conventional control algorithms have also been implemented using event-triggered sampling, for e.g. sliding mode control [19], model predictive control [20] etc. Many application based results such as ETC of networked power systems [21], networked unmanned aerial vehicle system [22], position tracking problem for a dc torque motor in [23] are established, to mention a few.

However, the ETC approaches used for normal systems can not be generalised for the SPSs. The main difficulty is the designing of the event-triggering condition and corresponding closed-loop system stability analysis, which is influenced by the singular perturbation parameter ϵ . The difficulties also include proving non-Zeno behaviour. Therefore, the study of SPSs under event-triggered sampling is significant from the theoretical and practical point of view, but very limited works have been reported in the literature for the ETC of SPSs. In [24], event-triggered feedback law is designed to stabilise only reduced-order slow model of a non-linear SPS. It is shown in [24] that the event-triggering rule derived by Lyapunov analysis does not eliminate the Zeno behaviour directly and therefore a variation like assimilating a constant threshold in the event-triggering rule or allowing transmissions only after a predefined amount of time after the latest transmission is proposed to overcome this issue. Event-triggered composite control is designed in [25], in which events are detected independently in slow and fast states which reduces the number of executions for the slow state. An ETC problem for synchronisation of non-linear singularly perturbed complex networks has been discussed in [26]. The event-triggered state estimation problem using a dynamic event-triggering threshold for a discrete-time SPS is taken up in [27]. An event-triggered H_∞ control problem for the discrete-time networked non-linear SPS is presented in [28]. In [29], event-triggered sliding mode control has been proposed for a discrete slow sampling model of SPS. It is worth mentioning that the Zeno effect is automatically ruled out in discrete systems.

In this paper, we investigate an ETC strategy for a networked SPS based on the sampling of its slow state only. An event-triggering mechanism (ETM) with an exponentially converging threshold [30, 31] is used that ensures a positive lower bound on the inter-event time, and thus eliminates the Zeno effect. The proposed control strategy guarantees asymptotic convergence to a small neighbourhood of the equilibrium point.

To validate the proposed control, it is applied on a laboratory-scale actual hardware setup of an active suspension system of a quarter car model. Dynamics of a vehicle suspension system comprises of two separate sets of fluctuating modes. The suspension system possesses a two-time-scale property and can be modelled as an SPS [32, 33]. In real applications of a vehicle suspension systems nowadays, the number of embedded sensors

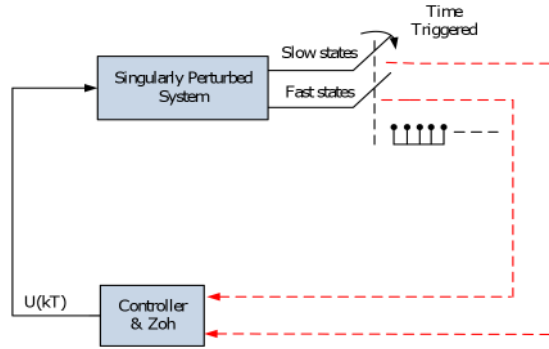


Fig. 1 Conventional sampled data control of SPS. Dotted line represents the communication through the network (periodic in this case). $U(kT)$ represents the control-input at k th sampling instant

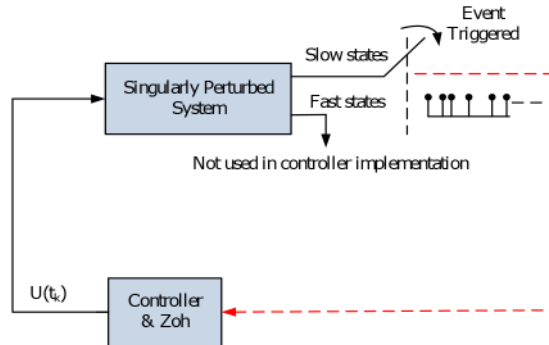


Fig. 2 Proposed ETC of SPS. Dotted line represents the communication through the network (aperiodic in this case). $U(t_k)$ represents the eventual control-input

and electronic control units are placed in a vehicle and transmission laws are customarily implemented on digital platforms and therefore ETC is well-motivated [34, 35]. Use of adaptive event-triggering conditions have been made for reliable control of the vehicle suspension system in [36] and non-linear vehicle active suspension systems with state constraints in [37]. In [38], an output-feedback based periodic ETC is designed for active suspension systems considering network-induced delays.

However, there are no experimental results available for ETC of the active suspension system. Experimental results obtained in this work indicate that in spite of the simplified structure of the controller and event-triggered feedback, its performance is comparable to that of the full-state feedback design with continuous feedback. Fig. 1 shows the conventional sampled-data control of an SPS with periodic sampling, whereas Fig. 2 shows the conceptual block diagram of the proposed reduced-order ETC of SPS.

The main contributions of this work are as follows:

- (1) ETC for an SPS is designed based only on its slow dynamics using an event-triggering condition that has exponentially converging threshold with time for ensuring the existence of a positive lower bound on the inter-event time.
- (2) The sufficient conditions for ensuring the stability of overall system are established. Lower bound on the inter-execution time is also calculated for various parameters of the event-triggering condition.
- (3) The proposed design is validated for a laboratory-scale set up of an active suspension system, which is modelled as an SPS. For an active suspension system, the proposed design has an advantage that only vehicle body measurements (slow modes) are required at the controller and not the tire measurements (fast modes) which are difficult to measure and ETC reduces the number of transmissions and control executions.

1.1 Notations

\mathbb{N}_0 is used to denote the set of natural numbers including zero. $\lambda(A)$ represents the eigenvalues of matrix A . $Re(\lambda(A))$ is the real part of the eigenvalues of A . Symbols $\lambda_{\max}(A)$ and $\lambda_{\min}(A)$ denote the largest

and the smallest eigenvalue of matrix A , respectively. $\|A\|$ denotes the induced-2 norm of the matrix $A \in \mathbb{R}^{n \times n}$ with $\|A\| = \sqrt{\lambda_{\max}(A^T A)}$. $\|x\|$ denotes Euclidean norm of vector $x \in \mathbb{R}^n$ with $\|x\| = \sqrt{x^T x}$. $\max\{\cdot\}$ and $\min\{\cdot\}$ represent the maximum value and minimum value, respectively. I_n is identity matrix of dimension $(n \times n)$. Superscript T represents the matrix transpose. x^0 represents initial condition on state $x(t)$. $|a|$ represents the absolute value of scalar a . O denotes Zero matrix of appropriate dimension. A vector function $f(t, \epsilon)$ is said to be $O(\epsilon)$ over an interval $[t_1, t_2]$ if there exist positive constants k and ϵ^* such that

$$\|f(t, \epsilon)\| \leq k\epsilon, \quad \forall \epsilon \in [0, \epsilon^*], \quad \forall t \in [t_1, t_2]$$

2 Preliminaries

Consider the following SPS with input $u(t)$

$$\dot{z}_1(t) = A_{11}z_1(t) + A_{12}z_2(t) + B_1u(t) \quad (1a)$$

$$\epsilon \dot{z}_2(t) = A_{21}z_1(t) + A_{22}z_2(t) + B_2u(t) \quad (1b)$$

where $z_1 \in \mathbb{R}^n$, $z_2 \in \mathbb{R}^m$ are slow and fast state, respectively. $u \in \mathbb{R}^p$ is an input and $\epsilon > 0$ is a small parameter. A_{11} , A_{12} , A_{21} and A_{22} are matrices of appropriate dimensions. We assume that A_{22}^{-1} exists and the system (1) is controllable.

2.1 Slow and fast subsystems

As $\epsilon \rightarrow 0$, the eigenvalues of SPS (1) cluster into a slow group of $O(1)$ eigenvalues and a fast group of $O(1/\epsilon)$ eigenvalues, and (4) has two-time scale structure. The full system can be approximated by the slow and fast subsystems provided A_{22}^{-1} exists [5]. By setting $\epsilon = 0$ in (1), we can obtain n th order slow subsystem as

$$\dot{z}_{1s}(t) = A_0 z_{1s}(t) + B_0 u_s(t), \quad z_{1s}(t_0) = z_1^0 \quad (2a)$$

$$z_{2s}(t) = -A_{22}^{-1}(A_{21}z_{1s}(t) + B_2u_s(t)) \quad (2b)$$

where

$$A_0 = A_{11} - A_{12}A_{22}^{-1}A_{21}, \quad B_0 = B_1 - A_{12}A_{22}^{-1}B_2, \quad (3)$$

and z_{1s}, z_{2s} and u_s denote the slow parts of z_1, z_2 and u , respectively, in the original system (1). The m th order fast subsystem is given by

$$\dot{z}_{2f}(\tau) = A_{22}z_{2f}(\tau) + B_2u_f(\tau), \quad z_{2f}(t_0) = z_2^0 - z_{2s}^0 \quad (4)$$

where $z_{2f} = z_2 - z_{2s}$ and $u_f = u - u_s$ denote the fast part of corresponding variables and τ is the fast time scale defined for all $\epsilon \geq 0$ by

$$\tau = \frac{t - t_0}{\epsilon}; \quad \tau = 0 \text{ at } t = t_0$$

Then the solution z_1, z_2 of the original system (1) is approximated for $\epsilon \in (0, \epsilon_1]$ by

$$z_1(t) = z_{1s}(t) + O(\epsilon) \quad (5a)$$

$$z_2(t) = -A_{22}^{-1}A_{21}z_1(t) + z_{2f}(\tau) + O(\epsilon) \quad (5b)$$

where ϵ_1 can be obtained as

$$\epsilon_1 = \left(\|A_{22}^{-1}\| \left(\|A_0\| + \|A_{12}\| \|A_{22}^{-1}A_{21}\| + 2(\|A_0\| \|A_{12}\| \|A_{22}^{-1}A_{21}\|)^{1/2} \right) \right)^{-1}$$

Various attributes of the SPS (1) including stability can also be approximated by its slow and fast dynamics (2)–(4) [2].

2.2 Composite control

Control laws can be designed to improve properties of each slow and fast subsystem. The total control law is obtained as a composite of the two control laws for the two subsystems provided the original system is controllable or systems in (2a) and (4) are stabilisable [4]. However, if the fast dynamics is stable, the feedback law can be designed only on the basis of approximate model of the slow dynamics. Assuming A_{22} to be a stable matrix, controller for (1) is designed so as to ensure that the slow system (2) is also stable. Controller $u_s = K_0 z_{1s}$ is designed such that matrix Λ_0 is stable, where

$$\Lambda_0 := A_0 + B_0 K_0 \quad (6)$$

So for system with stable fast dynamics, control input is given by $u = u_s$. Using (5), we replace z_{1s} by z_1 so that

$$u = K_0 z_1(t) \quad (7)$$

3 Problem formulation

This paper aims to stabilise the system (1) using a controller that is implemented over a network. The control law is based only on its slow state and sampling mechanism is event-triggered i.e. sampling instants are decided by some state dependent criterion. An emulation-based approach is followed, where controller is first designed without considering any communication constraints and later the effect of sampling is considered. So, we first design a controller as in (7) and assume the following:

Assumption 1: A_{22} is a Hurwitz matrix and the control gain K_0 is designed such that Λ_0 in (6) is a Hurwitz matrix.

With event-triggered sampling, the controller receives the measurements of state z_1 only at the transmission instants $\{t_k\}$, $k \in \mathbb{N}_0$ when an event occurs in state z_1 . Assuming zero-order-hold device at the input, input in (7) can be written as

$$u(t) = K_0 z_1(t_k), \quad \forall t \in [t_k, t_{k+1}) \quad (8)$$

where t_{k+1} is the next time instant when state measurement are released again to update the control (8). Defining measurement error as error between state at time t and the latest released values of state measurement as

$$z_e(t) = z_1(t_k) - z_1(t), \quad \forall t \in [t_k, t_{k+1}) \quad (9)$$

As $z_1(t_k)$ does not change between two consecutive executions of $z_1(t), \dot{z}_e(t)$ in this interval is given by

$$\dot{z}_e(t) = -\dot{z}_1(t), \quad \forall t \in [t_k, t_{k+1}) \quad (10)$$

Revising (1) in view of (8) and (9)

$$\dot{z}_1(t) = \Lambda_{11}z_1(t) + A_{12}z_2(t) + B_1 K_0 z_e(t) \quad (11a)$$

$$\epsilon \dot{z}_2(t) = \Lambda_{21}z_1(t) + A_{22}z_2(t) + B_2 K_0 z_e(t) \quad (11b)$$

where

$$\Lambda_{11} := A_{11} + B_1 K_0, \quad \Lambda_{21} := A_{21} + B_2 K_0.$$

(11) represents the dynamics of the overall closed loop system under event triggered sampling of its slow state. To implement the above ETC, a suitable ETM is required which can recursively determine the triggering instants for z_1 so as to ensure the stability of (11). Typically, whenever the norm of measurement error exceeds a predetermined threshold, an event is said to be triggered. In this work, the triggering function has a relative threshold which is progressively reduced as a function of the time. The successive release instances t_k for state z_1 are determined recursively as

$$t_{k+1} = \inf\{t: t > t_k \wedge (\|z_e(t)\| - (a_0 + a_1 e^{-\alpha t})) > 0\} \quad (12)$$

where α, a_0 and a_1 are design parameters such that $\alpha > 0, a_0 \geq 0$ and $a_1 \geq 0$, but both a_0 and a_1 can not be zero simultaneously.

Remark 1: If ($a_1 = 0$) ETM has fixed threshold, this type of ETM has been vastly studied in the literature of ETC [39, 40]. System state converges to a small region determined by a_0 around equilibrium point at the cost of the number of transmissions. If $a_0 = 0$, the threshold in ETM decreases purely exponentially and in this case system state asymptotically converges to the equilibrium point [31]. However, there is always a compromise between control performance and the number of executions. ETM in (12) is a combination of these two types of ETMs and performs well both in terms of the number of executions and control performance.

Remark 2: The time-dependent trigger function in (12) ensures asymptotic convergence to the equilibrium point while eliminating the Zeno behaviour even for distributed NCSs [41] or multiagent systems [30]. On the other hand, the most prevalent trigger functions in the literature are of the type $\|z_e(t)\| < \sigma \|z(t)\|$, which ensures asymptotic convergence to the equilibrium but existence of positive lower bound on inter event time may not be guaranteed, particularly in the case of partial state feedback [24], or for decentralised control [42]. The triggering rule in (12) gives better performance in terms of event generation when the system is close to the equilibrium [43].

Remark 3: It is inevitable that real-time detection and computation of the event-triggering scheme will induce computational burdens, but the energy to transmit 1 bit data is equivalent to 1000–3000 times of computational operations [44, 45], therefore saving in the communication resources obtained by using event-triggered mechanism is worth the extra computational burden.

4 Decoupling transformation

System (11) is in the standard singularly perturbed form where A_{22} is non-singular, then there exists an $\epsilon^* > 0$ such that for all

$0 < \epsilon < \epsilon^*$, a complete separation of (11) into block diagonal form can be achieved by a non-singular transformation matrix T , where

$$T = \begin{bmatrix} I_n & \epsilon H \\ -L & I_m - \epsilon LH \end{bmatrix} \quad (13a)$$

$$\text{with } T^{-1} = \begin{bmatrix} I_n - \epsilon HL & -\epsilon H \\ L & I_m \end{bmatrix} \quad (13b)$$

where matrices $L \in \mathbb{R}^{m \times n}$ and $H \in \mathbb{R}^{n \times m}$ satisfy the following linear algebraic equations

$$\Lambda_{21} - A_{22}L + \epsilon L\Lambda_{11} - \epsilon LA_{12}L = 0 \quad (14a)$$

$$A_{12} - HA_{22} + \epsilon\Lambda_{11}H - \epsilon A_{12}LH - \epsilon HLA_{12} = 0 \quad (14b)$$

Under the transformation

$$\begin{bmatrix} z_1(t) \\ z_2(t) \end{bmatrix} = T \begin{bmatrix} \xi(t) \\ \eta(t) \end{bmatrix} \quad (15)$$

The equivalent form of system (11) becomes

$$\begin{bmatrix} \dot{\xi}(t) \\ \epsilon \dot{\eta}(t) \end{bmatrix} = A_D \begin{bmatrix} \xi(t) \\ \eta(t) \end{bmatrix} + B_D K_0 z_e(t) \quad (16)$$

where $\xi(t)$ and $\eta(t)$ represent the exact slow and exact fast state vector of (11), respectively, and A_D is a block diagonal matrix with

$$A_D = \begin{bmatrix} \Lambda_s & O \\ O & \Lambda_f \end{bmatrix}, \quad B_D = \begin{bmatrix} B_s \\ B_f \end{bmatrix} \quad (17)$$

where

$$\begin{aligned} \Lambda_s &:= \Lambda_{11} - A_{12}L, \quad \Lambda_f := A_{22} + \epsilon LA_{12}, \\ B_s &:= B_1 - HB_2 - \epsilon HLB_1, \quad B_f := B_2 + \epsilon LB_1. \end{aligned} \quad (18)$$

After some algebraic manipulations, (not given here for conciseness), we can write for $O(\epsilon)$ approximations for $\epsilon \in (0, \epsilon^*]$:

$$L = A_{22}^{-1}\Lambda_{21} + O(\epsilon), \quad H = A_{12}A_{22}^{-1} + O(\epsilon), \quad (19a)$$

$$\Lambda_s = \Lambda_0 - \epsilon(A_{22}^{-1})^2\Lambda_{21}\Lambda_0 + O(\epsilon^2) = \Lambda_0 + O(\epsilon), \quad (19b)$$

$$\Lambda_f = A_{22} + \epsilon A_{22}^{-1}\Lambda_{21}A_{12} + O(\epsilon^2) = A_{22} + O(\epsilon), \quad (19c)$$

$$B_s = B_0 + O(\epsilon), \quad B_f = B_2 + O(\epsilon) \quad (19d)$$

so that,

$$A_D = \begin{bmatrix} \Lambda_0 & O \\ O & A_{22} \end{bmatrix} + O(\epsilon), \quad B_D = \begin{bmatrix} B_0 \\ B_2 \end{bmatrix} + O(\epsilon) \quad (20)$$

ϵ^* can be obtained as

$$\epsilon^* = \left(\left(\|A_{22}^{-1}\| \left(\| \Lambda_0 \| + \|A_{12}\| \|A_{22}^{-1}\Lambda_{21}\| \right) + 2 \left(\| \Lambda_0 \| \|A_{12}\| \|A_{22}^{-1}\Lambda_{21}\| \right)^{1/2} \right)^{-1} \right)$$

On substituting in (16), we have

$$\begin{aligned} \begin{bmatrix} \dot{\xi}(t) \\ \epsilon \dot{\eta}(t) \end{bmatrix} &= \begin{bmatrix} \Lambda_0 & O \\ O & A_{22} \end{bmatrix} \begin{bmatrix} \xi(t) \\ \eta(t) \end{bmatrix} \\ &+ \begin{bmatrix} B_0 \\ B_2 \end{bmatrix} K_0 z_e(t) + \begin{bmatrix} g_1(\xi, t, \epsilon) \\ g_2(\eta, t, \epsilon) \end{bmatrix} \end{aligned} \quad (21)$$

As Λ_0 and A_{22} are Hurwitz matrices, $g_1(\xi, t, \epsilon)$ and $g_2(\eta, t, \epsilon)$ are $O(\epsilon)$ vector functions such that $\|g_1(\xi, t, \epsilon)\| \leq d_1\epsilon$ and

$\|g_2(\eta, t, \epsilon)\| \leq d_2\epsilon$, where d_1 and d_2 are positive constants independent of ϵ . Since transformation matrix T is non-singular, stability of $[\xi^T \eta^T]$ implies stability of $[z_1^T z_2^T]$. Hence, we switch to (21) to prove the stability of (11).

5 Main results

Sufficient conditions for the stability properties of the closed-loop system (21) is characterised in the following theorem:

Theorem 1: For the event based closed-loop system (21), for $0 < \epsilon < \epsilon^0$, where $\epsilon^0 \in (0, \epsilon^*]$, with event-triggering conditions given by (12), the states of the system (21) starting from any bounded initial conditions ξ^0 and η^0 will remain in the $O(\epsilon)$ neighbourhood of the smallest invariant set containing φ , where φ is given by

$$\varphi := \left\{ \begin{bmatrix} \xi(t) \\ \eta(t) \end{bmatrix} \in \mathbb{R}^{n+m} : \| [\xi^T \eta^T] \| \leq \frac{\sqrt{\lambda_{\max}(P)} 2\sqrt{2}c\alpha_0}{\sqrt{\lambda_{\min}(P)} b} \right\} \quad (22)$$

$$\text{where } b = \min \{ \lambda_{\min}(Q_1), \lambda_{\min}(Q_2) \}; \quad (23a)$$

$$c = \max \{ \| P_1 B_0 K_0 \|, \| P_2 B_2 K_0 \| \} \quad (23b)$$

$$P = \begin{bmatrix} P_1 & O \\ O & \epsilon P_2 \end{bmatrix} \quad (23c)$$

P_1, P_2, Q_1 and Q_2 are positive definite symmetric matrices which satisfy the following Lyapunov equations

$$\Lambda_0^T P_1 + P_1 \Lambda_0 = -Q_1 \quad (24a)$$

$$A_{22}^T P_2 + P_2 A_{22} = -Q_2 \quad (24b)$$

Moreover for $\alpha < \beta_1$, Zeno effect is excluded and for $\epsilon \rightarrow 0$, inter-event times are lower-bounded by a strictly positive constant given by

$$t_e \geq \frac{\alpha_0}{(k_1 + k_2 + k_3 + k'_1 + k'_2 + k'_3)} \quad (25)$$

where k_1, k_2, k_3 and k'_1, k'_2, k'_3 are positive constants defined as

$$k_1 := \delta_1 \| \Lambda_0 \| \| \xi^0 \| \quad (26a)$$

$$k_2 := \| B_0 K_0 \| a_0 \left(1 + \frac{\delta_1 \| \Lambda_0 \|}{\beta_1} \right) \quad (26b)$$

$$k_3 := \| B_0 K_0 \| a_1 \left(1 + \frac{\delta_1 \| \Lambda_0 \|}{\beta_1 - \alpha} \right) \quad (26c)$$

$$k'_1 := \delta_2 \| H \| \| A_{22} \| \| \eta^0 \| \quad (26d)$$

$$k'_2 := \| H \| \| B_2 K_0 \| a_0 \left(1 + \frac{\delta_2 \| A_{22} \|}{\beta_2} \right) \quad (26e)$$

$$k'_3 := \| H \| \| B_2 K_0 \| a_1 \left(1 + \frac{\delta_2 \| A_{22} \|}{\beta_2 - \epsilon\alpha} \right) \quad (26f)$$

and

$$\beta_1 = \left| \max \{ \text{Re}(\lambda(\Lambda_0)) \} \right|, \quad \delta_1 = \| V_1 \| \| V_1^{-1} \| \quad (27)$$

$$\beta_2 = \left| \max \{ \text{Re}(\lambda(A_{22})) \} \right|, \quad \delta_2 = \| V_2 \| \| V_2^{-1} \| \quad (28)$$

V_1 and V_2 being the matrices of the eigen vectors of Λ_0 and A_{22} respectively, δ_1, β_1 and δ_2, β_2 are positive constants.

Proof: Let $V(z, t)$ be the Lyapunov function candidate for the system (21), such that

$$V(z, t) = \xi^T(t)P_1\xi(t) + \epsilon\eta^T(t)P_2\eta(t) \quad (29)$$

As Λ_0 and A_{22} are Hurwitz, then for any given positive definite, symmetric matrices Q_1 and Q_2 , there exist unique positive definite, symmetric matrices P_1 and P_2 which satisfy the Lyapunov equations given by (24a) and (24b), individually. The derivative of the function V along the flow of the closed loop system (21) is

$$\begin{aligned} \dot{V} = & \xi^T(\Lambda_0^T P_1 + P_1 \Lambda_0)\xi + \xi^T P_1 B_0 K_0 z_e + z_e^T K_0 B_0 P_1 \xi \\ & + \xi^T P_1 g_1(\xi, t, \epsilon) + g_1(\xi, t, \epsilon)^T P_1 \xi + \eta^T (A_{22}^T P_2 + P_2 A_{22})\eta \\ & + \eta^T P_2 B_2 K_0 z_e + z_e^T K_0 B_2 P_2 \eta + \eta^T P_2 g_2(\eta, t, \epsilon) + g_2(\eta, t, \epsilon)^T P_2 \end{aligned} \quad (30)$$

$$\begin{aligned} \dot{V} = & (-\xi^T Q_1 \xi + 2\xi^T P_1 B_0 K_0 z_e + 2\xi^T P_1 g_1(\xi, t, \epsilon)) \\ & + (-\eta^T Q_2 \eta + 2\eta^T P_2 B_2 K_0 z_e + 2\eta^T P_2 g_2(\eta, t, \epsilon)) \end{aligned} \quad (31)$$

$$\begin{aligned} \dot{V} = & -\xi^T Q_1 \xi - \eta^T Q_2 \eta + 2[\xi^T \eta^T] \begin{bmatrix} P_1 B_0 K_0 z_e \\ P_2 B_2 K_0 z_e \end{bmatrix} \\ & + 2[\xi^T \eta^T] \begin{bmatrix} P_1 g_1(\xi, t, \epsilon) \\ P_2 g_2(\eta, t, \epsilon) \end{bmatrix} \end{aligned} \quad (32)$$

Making use of the following property of any positive definite matrix Q :

$$\lambda_{\min}(Q) \|x(t)\|^2 \leq x(t)^T Q x(t) \leq \lambda_{\max}(Q) \|x(t)\|^2$$

The right-hand side of (32) can be bounded as

$$\begin{aligned} \dot{V} \leq & -\lambda_{\min}(Q_1) \|\xi\|^2 - \lambda_{\min}(Q_2) \|\eta\|^2 \\ & + 2 \|\xi^T \eta^T\| \|z_e\| \sqrt{\|P_1 B_0 K_0\|^2 + \|P_2 B_2 K_0\|^2} \\ & + 2 \|\xi^T \eta^T\| \epsilon \sqrt{\|d_1 P_1\|^2 + \|d_2 P_2\|^2} \end{aligned} \quad (33)$$

The ETM in (12) enforces $\|z_e(t)\| \leq (a_0 + a_1 e^{-\alpha t})$, so that

$$\begin{aligned} \dot{V} \leq & -b \|\xi^T \eta^T\|^2 + 2\sqrt{2}c(a_0 + a_1 e^{-\alpha t}) \|\xi^T \eta^T\| \\ & + 2\sqrt{2}d\epsilon \|\xi^T \eta^T\| \end{aligned} \quad (34)$$

where b and c are as defined in (23), and $d = \max\{\|d_1 P_1\|, \|d_2 P_2\|\}$. For $\epsilon \in (0, \epsilon^0]$, where $\epsilon^0 \in (0, \epsilon^*)$ is sufficiently small such that $2\sqrt{2}d\epsilon$ is $O(\epsilon)$. \square

$$\dot{V} \leq -b \|\xi^T \eta^T\| \left(\|\xi^T \eta^T\| - \frac{2\sqrt{2}c(a_0 + a_1 e^{-\alpha t})}{b} - O(\epsilon) \right)$$

$$\dot{V} < 0 \quad \forall \quad \|\xi^T \eta^T\| > \frac{2\sqrt{2}c(a_0 + a_1 e^{-\alpha t})}{b} + O(\epsilon) \quad (35)$$

As $t \rightarrow \infty$,

$$\dot{V} < 0 \quad \forall \quad \|\xi^T \eta^T\| > \frac{2\sqrt{2}ca_0}{b} + O(\epsilon) \quad (36)$$

Applying Theorem 4.18 of [46], it can be shown that states $[\xi(t)^T \eta(t)^T]$ remain ultimately bounded to the $O(\epsilon)$ neighbourhood of the set given by (22). This proves the first part of Theorem 1.

To obtain lower bound on inter-event time, we first solve state (21). The norm of states can be bounded as

$$\begin{aligned} \|\xi(t)\| \leq & \|e^{\Lambda_0 t}\| \|\xi^0\| + \int_0^t \|e^{\Lambda_0(t-s)}\| \|B_0 K_0\| \|z_e(s)\| ds \\ & + \int_0^t \|e^{\Lambda_0(t-s)}\| \|g_1(\xi, t, \epsilon)\| ds \end{aligned} \quad (37a)$$

$$\begin{aligned} \|\eta(t)\| \leq & \|e^{(A_{22}/\epsilon)t}\| \|\eta^0\| \\ & + \frac{1}{\epsilon} \int_0^t \|e^{(A_{22}/\epsilon)(t-s)}\| \|B_2 K_0\| \|z_e(s)\| ds \\ & + \frac{1}{\epsilon} \int_0^t \|e^{(A_{22}/\epsilon)(t-s)}\| \|g_2(\eta, t, \epsilon)\| ds \end{aligned} \quad (37b)$$

By assumption, A_{22} is Hurwitz and by design of controller, Λ_0 is also Hurwitz, hence

$$\|e^{\Lambda_0 t}\| \leq \delta_1 e^{-\beta_1 t} \quad \text{and} \quad \|e^{A_{22} t}\| \leq \delta_2 e^{-\beta_2 t}$$

$$\begin{aligned} \|\xi(t)\| \leq & \delta_1 e^{-\beta_1 t} \|\xi^0\| + \int_0^t \delta_1 e^{-\beta_1(t-s)} \|B_0 K_0\| (a_0 + a_1 e^{-\alpha s}) ds \\ & + \int_0^t \delta_1 e^{-\beta_1(t-s)} d_1 \epsilon ds \end{aligned} \quad (38a)$$

$$\begin{aligned} \|\eta(t)\| \leq & \delta_2 e^{(-\beta_2/\epsilon)t} \|\eta^0\| \\ & + \frac{\delta_2}{\epsilon} \int_0^t e^{(-\beta_2/\epsilon)(t-s)} \|B_2 K_0\| (a_0 + a_1 e^{-\alpha s}) ds \\ & + \frac{\delta_2}{\epsilon} \int_0^t e^{(-\beta_2/\epsilon)(t-s)} d_2 \epsilon ds \end{aligned} \quad (38b)$$

By integrating and combining terms, it follows that

$$\begin{aligned} \|\xi(t)\| \leq & \delta_1 \|\xi^0\| e^{-\beta_1 t} + \frac{\delta_1 \|B_0 K_0\| a_0}{\beta_1} (1 - e^{-\beta_1 t}) \\ & + \frac{\delta_1 \|B_0 K_0\| a_1}{\beta_1 - \alpha} (e^{-\alpha t} - e^{-\beta_1 t}) + \frac{\delta_1 \epsilon d_1}{\beta_1} (1 - e^{-\beta_1 t}) \end{aligned} \quad (39a)$$

$$\begin{aligned} \|\eta(t)\| \leq & \delta_2 \|\eta^0\| e^{(-\beta_2/\epsilon)t} + \frac{\delta_2 \|B_2 K_0\| a_0}{\beta_2} (1 - e^{(-\beta_2/\epsilon)t}) \\ & + \frac{\delta_2 \|B_2 K_0\| a_1}{\beta_2 - \epsilon\alpha} (e^{-\alpha t} - e^{(-\beta_2/\epsilon)t}) + \frac{\delta_2 \epsilon d_2}{\beta_2} (1 - e^{(-\beta_2/\epsilon)t}) \end{aligned} \quad (39b)$$

We can further upper bound the norm of states as shown in (40) and (41).

(see (40))

(see (41))

To calculate the inter execution time, we use the fact that the minimum time between events is the time it takes for $\|z_e(t)\|$ to grow from 0 at $t = t_k$ to $\|z_e(t)\| = (a_0 + a_1 e^{-\alpha t})$ at $t = t_{k+1}$. We need to prove the existence of an upper bound on the rate of change of $\|z_e(t)\|$. As $(d/dt) \|z_e\| \leq \|z_e\|$ and from (10) between two consecutive events $\|\dot{z}_e(t)\| = \|\dot{z}(t)\|$. In view of (13) and (15), $\|\dot{z}_e(t)\| = \|\dot{\xi}(t) + \epsilon H\dot{\eta}(t)\|$ or $\|\dot{z}_e(t)\| \leq \|\dot{\xi}(t)\| + \|\epsilon H\dot{\eta}(t)\|$ and therefore, $\forall t \in [t_k, t_{k+1})$

$$\|\xi(t)\| \leq \frac{\delta_1}{\beta_1} (\|B_0 K_0\| a_0 + \epsilon d_1) + \delta_1 \|\xi^0\| e^{-\beta_1 t} + \frac{\delta_1 \|B_0 K_0\| a_1}{\beta_1 - \alpha} e^{-\alpha t} \quad (40)$$

$$\|\eta(t)\| \leq \frac{\delta_2}{\beta_2} (\|B_2 K_0\| a_0 + \epsilon d_2) + \delta_2 \|\eta^0\| e^{(-\beta_2/\epsilon)t} + \frac{\delta_2 \|B_2 K_0\| a_1}{\beta_2 - \epsilon\alpha} e^{-\alpha t} \quad (41)$$

$$\begin{aligned} \frac{d}{dt} \|z_e\| &\leq \| \dot{z}_e \| \leq \| \Lambda_0 \| \| \xi(t) \| + \| B_0 K_0 \| (a_0 + a_1 e^{-\alpha t}) \\ &+ \| g_1(\xi, t, \epsilon) \| + \| H \| \| A_{22} \| \| \eta(t) \| \\ &+ \| H \| \| B_2 K_0 \| (a_0 + a_1 e^{-\alpha t}) + \| H \| \| g_2(\xi, t, \epsilon) \| \end{aligned} \quad (42)$$

If the latest event for state x_1 occurs at time $t_k \geq 0$ then $\forall t \in [t_k, t_{k+1})$, $\| \xi(t) \| \leq \| \xi(t_k) \|$ and $\| \eta(t) \| \leq \| \eta(t_k) \|$ hold in (40) and (41), respectively. So that (42) can be written as (see (43))

On integrating both sides from t_k to t and realising that $z_e(t_k) = 0$, we get (44), (44) can be further written as (45) by making use of (40) and (41).

(see (44))

(see (45))

By defining k_1, k_2, k_3 and k'_1, k'_2, k'_3 as in (26), we can deduce (46) from (45) (see (46)), where

$$D := \left(1 + \frac{\| \Lambda_0 \|}{\beta_1}\right) d_1 + \left(\| H \| + \frac{\| H A_{22} \|}{\beta_2}\right) d_2$$

For sufficiently small ϵ^0 , $D\epsilon$ is $O(\epsilon)$, and the quantity in bracket in (46) can further be upper bounded as $(k_1 + k_2 + k_3 + k'_1 + k'_2 + k'_3 + |O(\epsilon)|)$. k_1, k_2, k_3 and k'_1, k'_2, k'_3 are positive constants provided $\beta_1 > \alpha$. Therefore,

$$\|z_e(t)\| \leq (k_1 + k_2 + k_3 + k'_1 + k'_2 + k'_3 + |O(\epsilon)|)(t - t_k) \quad (47)$$

The next execution takes place when $\|z_e(t)\| = a_0 + a_1 e^{-\alpha t} \geq a_0$. Thus inter-execution time $t_e = (t_{k+1} - t_k)$ is given by

$$t_e \geq \frac{a_0}{(k_1 + k_2 + k_3 + k'_1 + k'_2 + k'_3 + |O(\epsilon)|)} \quad (48)$$

(48) shows that inter-execution time t_e is a positive quantity and is valid for all event times and this proves that Zeno behaviour is eliminated. As $\epsilon \rightarrow 0$, a lower bound t_e on the inter-execution time $(t_{k+1} - t_k)$ can be estimated by (25) and is valid for all event times. This proves the theorem.

5.1 Asymptotic stability

Next, we consider a specific case when $a_0 = 0$ and $a_1 \neq 0$ in (12). The event-triggering threshold is purely exponential and error is delimited by $\|z_e(t)\| \leq a_1 e^{-\alpha t}$. We can revise (22) for this case by

substituting $a_0 = 0$ which confirms that system state approaches an $O(\epsilon)$ neighbourhood of origin as $t \rightarrow \infty$.

To determine the time between two successive transmissions, we re-evaluate (46) for $k_2 = 0$ and $k'_2 = 0$ for $t > t_k$

$$\|z_e(t)\| \leq \int_{t_k}^t (k_1 e^{-\beta_1 t_k} + k_3 e^{-\alpha t_k} + k'_1 e^{-(\beta_2/\epsilon)t_k} + k'_3 e^{-\alpha t_k} + |O(\epsilon)|) ds \quad (49)$$

Next event can not be triggered before $\|z_e(t)\| = a_1 e^{-\alpha t}$.

$$a_1 e^{-\alpha t} = \int_{t_k}^t (k_1 e^{-\beta_1 t_k} + k_3 e^{-\alpha t_k} + k'_1 e^{-(\beta_2/\epsilon)t_k} + k'_3 e^{-\alpha t_k} + |O(\epsilon)|) ds$$

Minimum bound on the inter-event time can be obtained by the solution of above equation for $t_e = t - t_k$. On simplifying further,

$$(k_1 e^{(\alpha - \beta_1)t_k} + k_3 + k'_1 e^{(\alpha - (\beta_2/\epsilon)t_k} + k'_3 + |O(\epsilon)|) e^{\alpha t_k}) t_e = a_1 e^{-\alpha t_e} \quad (50)$$

The right hand side of (50) is always positive. Moreover, for $\alpha < \beta_1$, the bracketed quantity in left hand side is also positive with the upper and lower bound as $k_1 + k_3 + k'_1 + k'_3 + |O(\epsilon)|$ and $k_3 + k'_3 + |O(\epsilon)|$ respectively, and this produces a positive value of t_e for all $t_k \geq 0$. The inter event times are greater or equal to t_e given by $(k_1 + k_3 + k'_1 + k'_3 + |O(\epsilon)|) t_e = a_1 e^{-\alpha t_e}$ which is strictly positive. This proves the admissibility of exponential trigger function.

Remark 4: For simplicity, any time delay between sensing, transmission, computation and actuation instants has not been considered. However, in real-practice delays are always present. Calculation of lower bound on the inter-event time gives us an estimation of the delay one can account for, in the system.

6 Active suspension system

The quarter car model of active suspension system can be modelled as a double mass-spring-damper system with two inputs as shown in Fig. 3. Body displacement is denoted by z_s and z_{us} represents the tire position. The first input is the force $F_c(t)$ which is applied between the body and wheel assembly. This can be controlled by the feedback and represents the active component of the suspension system. The second system input is the derivative of road surface position $z_r(t)$. The state vector is defined as

$$\begin{aligned} \frac{d}{dt} \|z_e\| &\leq \| \Lambda_0 \| \| \xi(t_k) \| + \| H \| \| A_{22} \| \| \eta(t_k) \| + \epsilon(d_1 + \| H \| d_2) \\ &+ (\| B_0 K_0 \| + \| H \| \| B_2 K_0 \|)(a_0 + a_1 e^{-\alpha t_k}) \end{aligned} \quad (43)$$

$$\begin{aligned} \|z_e(t)\| &\leq \int_{t_k}^t (\| \Lambda_0 \| \| \xi(t_k) \| + \| H \| \| A_{22} \| \| \eta(t_k) \| + \epsilon(d_1 + \| H \| d_2) \\ &+ (\| B_0 K_0 \| + \| H \| \| B_2 K_0 \|)(a_0 + a_1 e^{-\alpha t_k})) ds \end{aligned} \quad (44)$$

$$\begin{aligned} \|z_e(t)\| &\leq \int_{t_k}^t \left(\| \Lambda_0 \| \left(\delta_1 \| \xi^0 \| e^{-\beta_1 t_k} + \frac{\delta_1 \| B_0 K_0 \| a_0 + \epsilon d_1}{\beta_1} + \frac{\delta_1 \| B_0 K_0 \| a_1}{\beta_1 - \alpha} e^{-\alpha t_k} \right) \right. \\ &+ \| H \| \| A_{22} \| \left(\delta_2 \| \eta^0 \| e^{-(\beta_2/\epsilon)t_k} + \frac{\delta_2 \| B_2 K_0 \| a_0 + \epsilon d_2}{\beta_2} + \frac{\delta_2 \| B_2 K_0 \| a_1}{\beta_2 - \epsilon \alpha} e^{-\alpha t_k} \right) \\ &\left. + \epsilon(d_1 + d_2 \| H \|) + (\| B_0 K_0 \| + \| H \| \| B_2 K_0 \|)(a_0 + a_1 e^{-\alpha t_k}) \right) ds \end{aligned} \quad (45)$$

$$\|z_e(t)\| \leq \int_{t_k}^t (k_1 e^{-\beta_1 t_k} + k_2 + k_3 e^{-\alpha t_k} + k'_1 e^{-(\beta_2/\epsilon)t_k} + k'_2 + k'_3 e^{-\alpha t_k} + D\epsilon) ds, \quad (46)$$

$$x = \begin{bmatrix} x_1(t) \\ x_2(t) \\ x_3(t) \\ x_4(t) \end{bmatrix} = \begin{bmatrix} z_s - z_{us} \\ \dot{z}_s \\ z_{us} - z_r \\ \dot{z}_r \end{bmatrix} \quad (51)$$

$x_1(t)$ is the suspension travel, $x_2(t)$ is the vehicle body vertical velocity, $x_3(t)$ represents the tire deflection and $x_4(t)$ is the wheel vertical velocity. The input, $\dot{z}_r(t)$ is the road surface velocity and the corresponding input vector is E and input $F_c(t)$ is the control action and B is the related input vector. The equations of motion of the system can be described in the state space as

$$\dot{x} = Ax + BF_c(t) + E\dot{z}_r(t) \quad (52)$$

The matrices A , B , E are given as

$$A = \begin{bmatrix} 0 & 1 & 0 & -1 \\ -\frac{K_s}{M_s} & -\frac{B_s}{M_s} & 0 & \frac{B_s}{M_s} \\ 0 & 0 & 0 & 1 \\ \frac{K_s}{M_{us}} & \frac{B_s}{M_{us}} & -\frac{K_{us}}{M_{us}} & -\frac{B_s + B_{us}}{M_{us}} \end{bmatrix} \quad (53)$$

$$B = \begin{bmatrix} 0 \\ \frac{1}{M_s} \\ 0 \\ -\frac{1}{M_{us}} \end{bmatrix}, \quad E = \begin{bmatrix} 0 \\ 0 \\ -1 \\ \frac{B_{us}}{M_{us}} \end{bmatrix} \quad (54)$$

K_s represents spring stiffness between car body and tire, B_s is damping coefficient between car body and tire. M_s represents the car chassis (body) mass. K_{us} denotes spring stiffness between tire and road. B_{us} is damping coefficient between tire and road. M_{us} represents the wheel assembly (Tire mass).

Remark 5: The equilibrium point of state space is assumed to be $x_1(t) = 0$ and $x_2(t) = 0$. However, in actual practice, springs are never relaxed due to weight of masses M_s and M_{us} . In other words due to gravity, equilibrium point of x_1 , x_2 does not collocate with location where springs are relaxed.

6.1 Active suspension as singularly perturbed system

In a typical suspension system, the ratio of the magnitude of the eigenvalues which correlate with the unsprung mass (wheel hop mode) ($|\lambda_f|$) to that which associate with the sprung mass (rigid

body mode) ($|\lambda_s|$) is almost of the order of ten and frequency response of the vehicle suspension system reflects two distinct resonant frequencies. The suspension system displays a two-time-scale property, with its body mode as slow mode and and the wheel hop mode as fast mode. The ratio of $\max\{|\lambda_s|\}$ to $\min\{|\lambda_f|\}$ is taken as the approximate value of the singular perturbation parameter ϵ without any loss of generality.

In order to find suitable controller for an active suspension system by making use of two-time scale property of the system, (52) is partitioned as

$$\dot{X}_1 = A_{11}X_1 + A_{12}X_2 + B_1F_c \quad (55a)$$

$$\dot{X}_2 = \hat{A}_{21}X_1 + \hat{A}_{22}X_2 + \hat{B}_2F_c \quad (55b)$$

where

$$X_1 = [x_1 \quad x_2]^T; \quad X_2 = [x_3 \quad x_4]^T; \quad A_{11} = \begin{bmatrix} 0 & 1 \\ -\frac{K_s}{M_s} & -\frac{B_s}{M_s} \end{bmatrix}$$

$$A_{12} = \begin{bmatrix} 0 & -1 \\ 0 & \frac{B_s}{M_s} \end{bmatrix}; \quad \hat{A}_{21} = \begin{bmatrix} 0 & 0 \\ \frac{K_s}{M_{us}} & \frac{B_s}{M_{us}} \end{bmatrix}$$

$$\hat{A}_{22} = \begin{bmatrix} 0 & 1 \\ -\frac{K_{us}}{M_{us}} & -\frac{(B_s + B_{us})}{M_{us}} \end{bmatrix}; \quad B_1 = \begin{bmatrix} 1 \\ \frac{1}{M_s} \end{bmatrix}; \quad \hat{B}_2 = \begin{bmatrix} 0 \\ -\frac{1}{M_{us}} \end{bmatrix}$$

Note that input $\dot{z}_r(t)$ is ignored to design the control law. To express the system (52) in the standard singularly perturbed form as in (1), we designate x_1 and x_2 as slow variables and x_3 and x_4 as fast variables and denote singular perturbation parameter $\epsilon = \min\{|\lambda(A)|\} / \max\{|\lambda(A)|\}$, the standard singular perturbation form of (52) is then given by

$$\dot{X}_1 = A_{11}X_1 + A_{12}X_2 + B_1F_c \quad (56a)$$

$$\epsilon\dot{X}_2 = A_{21}X_1 + A_{22}X_2 + B_2F_c \quad (56b)$$

where $A_{21} = \epsilon\hat{A}_{21}$; $A_{22} = \epsilon\hat{A}_{22}$; $B_2 = \epsilon\hat{B}_2$.

7 Experimental results

To validate the proposed control, the controller is implemented on an actual hardware setup of a bench-scale model shown in Fig. 4 to emulate a quarter-car model, controlled by active suspension mechanism. Model parameters of this system are listed in Table 1. The experimental setup comprises of three masses in the form of plates, which can move in a vertical direction independent of each

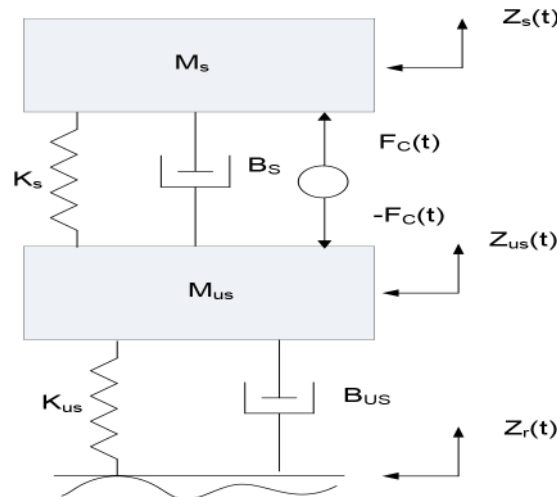


Fig. 3 Structure of active suspension system

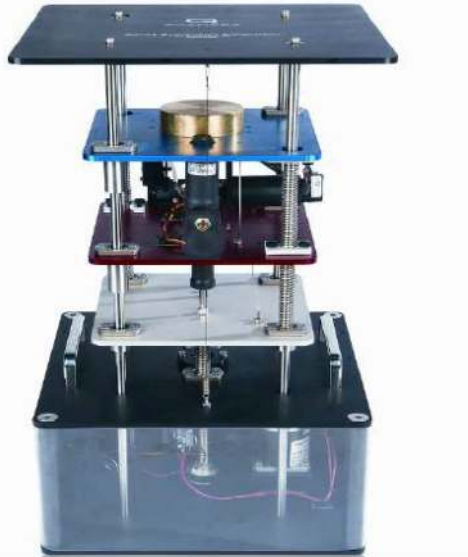


Fig. 4 Quarter-car active suspension setup in the lab

Table 1 The physical parameters of active suspension setup [47]

Symbol	Value	Symbol	Value
K_s	900 N/m	K_{us}	2500 N/m
B_s	7.5 Ns/m	B_{us}	5 Ns/m
M_s	2.45 kg	M_{us}	1.0 kg

other. For generating different road profiles a fast response brushed DC servo motor is used which drives the bottom plate. The middle plate represents the unsprung mass and is linked to the bottom plate by a spring and a damper. The top plate represents the sprung mass (vehicle body) supported above the suspension and it is connected to the middle plate by a spring, damper and a high-quality DC motor through a capstan. This capstan arrangement can generate motion in both the directions and known as the actuator of the control system that can dynamically compensate for the perturbations induced by the road and the setup mimics as the active suspension system. In this setup, 10-bit optical encoders are used to sense the positions of the sprung and unsprung masses and their velocities are obtained by high pass filters [47].

In order to apply the singular perturbation theory, we first verify the two-time-scale property of this system. For that we calculate the eigenvalues of matrix A using the parameters given in Table 1, which come out to be $[-6.9453 \pm 58.7246i, -0.8353 \pm 16.1843i]$. It is seen that two sets of eigenvalues are well separated. We calculate $\epsilon = 0.27$ (see Remark 6). The parameters of approximate slow and fast subsystems are given as

Slow subsystem parameters

$$A_0 = \begin{bmatrix} 0 & 1.0 \\ -367.3469 & -3.0612 \end{bmatrix}, \quad B_0 = \begin{bmatrix} 0 \\ 0.4082 \end{bmatrix} \quad (57)$$

Fast subsystem parameters

$$A_{22} = \begin{bmatrix} 0 & 0.27 \\ -675 & -3.375 \end{bmatrix}, \quad B_2 = \begin{bmatrix} 0 \\ -0.27 \end{bmatrix} \quad (58)$$

It can be seen that eigenvalues of A_{22} are $[-2.5500 \pm 20.0414i]$, and the fast subsystem is sufficiently stable. Therefore, control is designed only for the slow system and control gain is calculated by optimising the following performance index $J = \int_0^\infty (z_1^T S_1 z_1 + u^2 R) dt$

$$S_1 = \begin{bmatrix} 450 & 0 \\ 0 & 30 \end{bmatrix}, \quad R = 0.01 \quad (59)$$

so that $K_0 = [-24.6621 \quad -48.8657]$. The control law in (8) is tested for the hardware setup in Fig. 4 using ETM in (12) with $a_0 = 0.01$, $a_1 = 0.01$ and $\alpha = 0.3$. For the comparison purpose, a full state linear quadratic regulator (LQR) control proposed in [47] is used. In this approach, the performance parameters as well as actuator limitations are quantified in a quadratic measure given by

$$J = \int_0^\infty (x^T S x + u^2 R) dt$$

where $x(t)$ denotes the actual state of the system and $u(t)$ is the actual control input.

$$S = \begin{bmatrix} 450 & 0 & 0 & 0 \\ 0 & 30 & 0 & 0 \\ 0 & 0 & 5 & 0 \\ 0 & 0 & 0 & 0.01 \end{bmatrix}, \quad R = 0.01 \quad (60)$$

So that $u(t) = -Kx(t)$ and

$$K = [24.6621 \quad 48.8773 \quad -0.4712 \quad 3.6848] \quad (61)$$

Both the controllers are implemented in real-time using Matlab/Simulink environment with 1 ms sampling time for an acceptable accuracy. In an active-suspension system, road profile is usually interpreted as external disturbance. In this experiment, we use two types of road profiles (z_r) to validate the proposed ETC.

Road profile I: z_r is rectangular pulse of 20 mm height and 3 s period with 50% duty cycle.

Figs. 5a–c show the suspension travel, tire deflection and the vertical acceleration of the vehicle body, respectively, for the the proposed ETC and full state LQR control in (61). Plots of body position z_s and tire position z_{us} plotted over road surface position z_r for the proposed ETC are depicted in the Fig. 5d. Control input and the release instants under event-triggered scheme are shown in Figs. 6a and b respectively. It can be observed that response of the proposed ETC gives almost similar response to that given by full state LQR control with very less triggering instants, only 71 in 3 s. Minimum inter-event time is calculated as 3 ms. The difference in settling position of tire and body in Fig. 5d can be accounted for the reasons given in Remark 5. Although for better road handling properties, one can design a composite controller for both slow and fast systems. Its easy to imagine that number of transmissions will

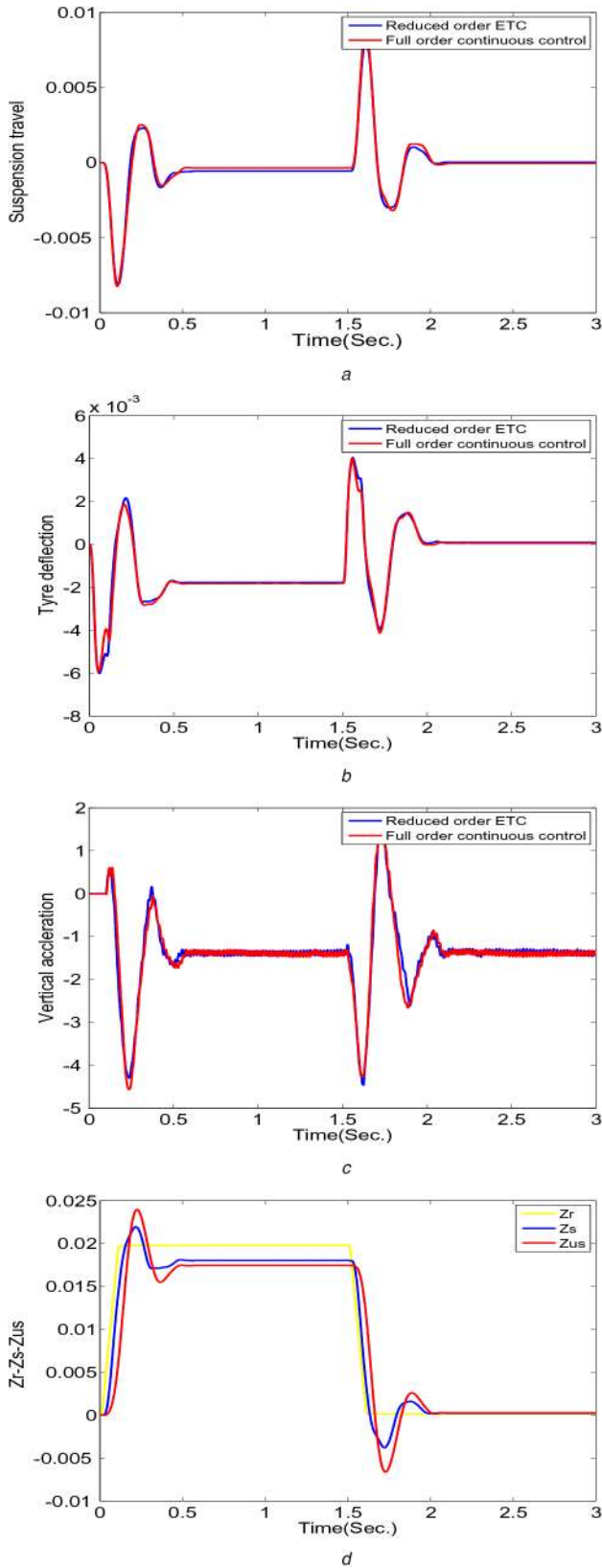


Fig. 5 Experimental results for road profile I
(a) Suspension travel (m), (b) Tyre deflection (m), (c) Vertical acceleration of sprung mass (m/s^2), (d) Z_r , Z_s and Z_{us} in (m) for the proposed ETC

increase in that case due to feedback of fast state. Control input in ETC system is piece-wise constant as shown in Fig. 6a.

Road profile II: Sine wave of 3 Hz frequency and 10 mm amplitude, i.e. $z_r = 0.01\sin(6\pi t)$.

Figs. 7 and 8 show the responses for road profile II. It can be observed that response of the proposed event-triggered controller gives almost similar response to that given by full state LQR

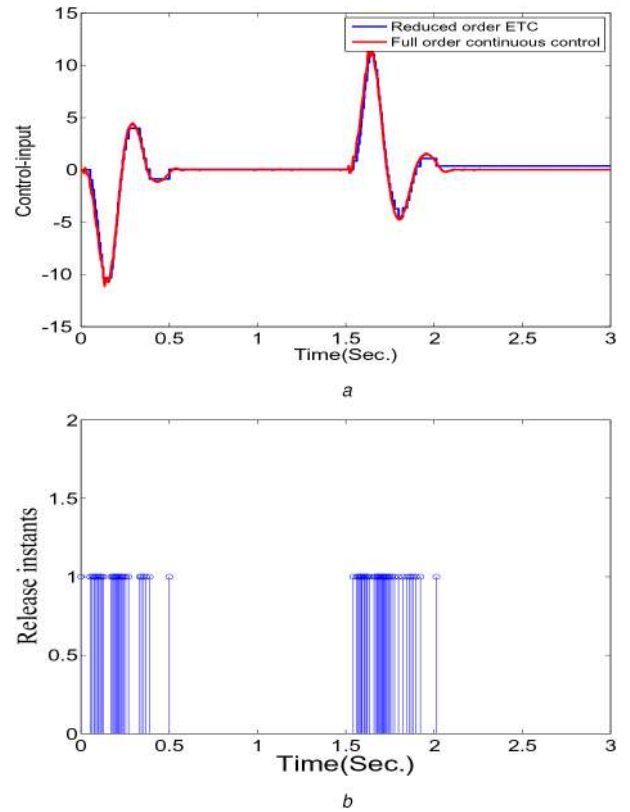


Fig. 6 Control input and release instants for road profile I in the proposed ETC

(a) Control input N , (b) Release instants

controller with 465 transmissions in 2 s. Control input is piece-wise constant as shown in Fig. 8a. It can be noticed that the proposed controller can stabilise the system even in the presence of extreme road condition, i.e. sinusoidal type of road profile.

Remark 6: This setup is the laboratory-scale model to emulate a quarter-car model and ratio of sprung mass M_s to unsprung mass M_{us} is not that high compared to any actual vehicle suspension system. Therefore, ϵ is also not very small for this system.

Remark 7: Practically, measurement of tyre deflection is a difficult task and also controlling fast modes (unsprung mass) requires a great deal of energy. By means of the singular perturbation method, we can give reduced-order feedback such that neither the tyre deflection nor the wheel velocity is fed back in this control law. This is an advantage over the full-state feedback law.

Remark 8: The efficacy of using singular perturbation theory for the analysis of active suspension system may not be apparent for a simple problem of quarter car model, but in an extended problem such as full car model, where a high-order controller is impractical in most situations, better and greater advantages of using singular perturbation theory are reflected.

8 Conclusion

This paper investigates a reduced-order event-triggered controller for a linear SPS based only on its slow dynamics. The proposed ETM guarantees that the system trajectories asymptotically converge towards a small neighbourhood of equilibrium point without exhibiting Zeno behaviour. The contribution of the paper has been verified by applying it on a laboratory scale actual hardware setup of an active suspension system of the quarter car model. The findings of this paper pave a way for the following problems to be further investigated:

- Network induced delays and quantisation are inevitable in digital networks. The proposed method can be extended to study event-

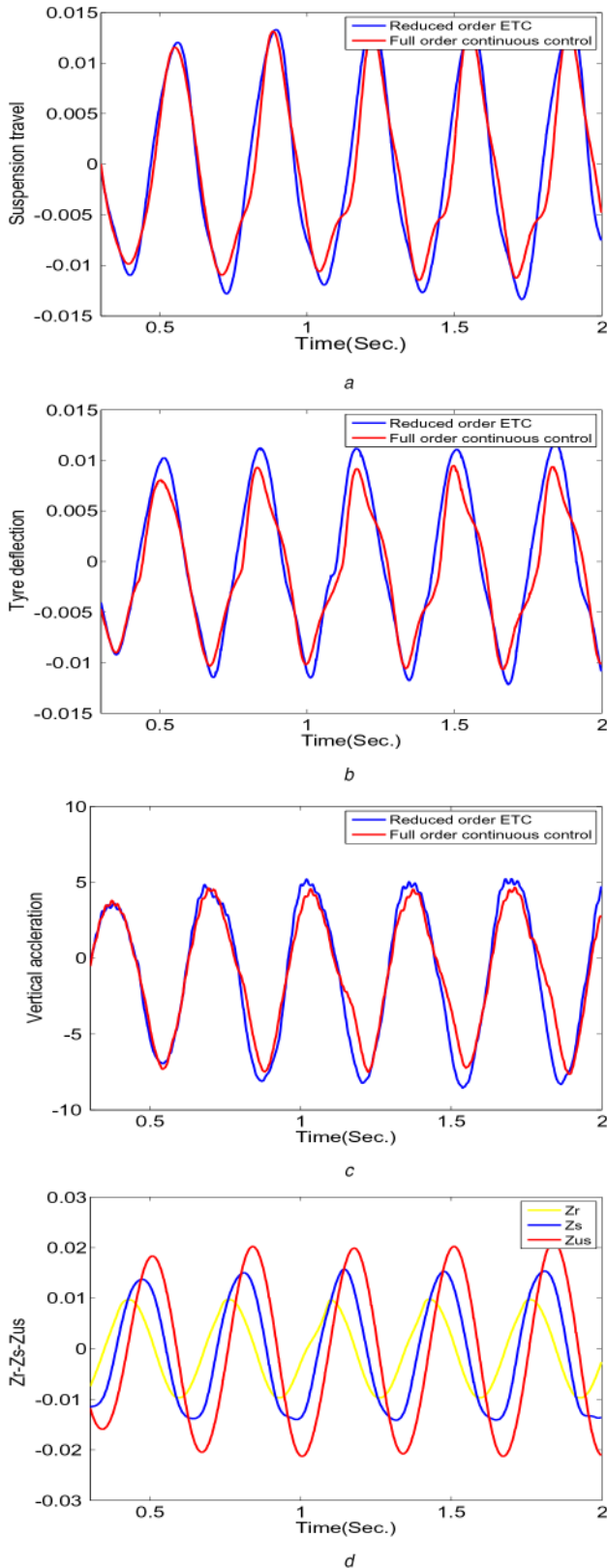


Fig. 7 Experimental results for road profile II
 (a) Suspension travel (m), (b) Tyre deflection (m), (c) Vertical acceleration of sprung mass (m/s^2), (d) Z_r , Z_s and Z_{us} in (m) for the proposed ETC

triggered stabilisation of SPS under bounded bit rates and with network induced delays.

• Many practical engineering systems can be modelled as SPSs, for e.g. air flight control systems, multi-link flexible robot, dc-dc power converters, synchronous machines, power-systems etc. (see [1] and references therein). Model order reduction in these systems is extremely helpful and it will be interesting to apply the proposed idea in this work for reduced-order ETC of these systems.

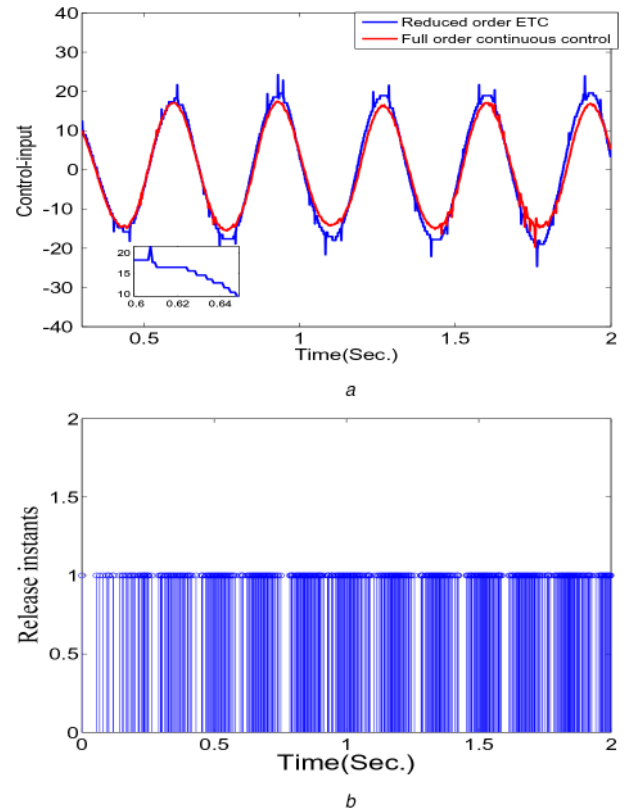


Fig. 8 Control input and release instants for road profile II in the proposed ETC
 (a) Control input N , (b) Release instants in proposed ETC

• By integrating the idea in this paper, ETC could be realised through some novel event-triggering conditions which can ensure stability and can avoid infinitely fast sampling and at the same time can improve results by reducing the number of transmissions.

9 References

- [1] Zhang, Y., Naidu, D.S., Cai, C., *et al.*: 'Singular perturbation and time scales in control theories and applications: an overview 2002–2012', *Int. J. Inf. Syst. Sci.*, 2014, **9**, (1), pp. 1–36
- [2] Kokotović, P., Khalil, H.K., O'Reilly, J.: 'Singular perturbation methods in control: analysis and design' (SIAM, 1999) <https://doi.org/10.1137/1.9781611971118>
- [3] Naidu, D.S.: 'Singular perturbation methodology in control systems' (IET, UK, 1988), 34
- [4] Suzuki, M., Miura, M.: 'Stabilizing feedback controllers for singularly perturbed linear constant systems', *IEEE Trans. Autom. Control*, 1976, **21**, (1), pp. 123–124
- [5] Kokotovic, P.V., O'Malley, Jr.R.E., Sannuti, P.: 'Singular perturbations and order reduction in control theory: an overview', *Automatica*, 1976, **12**, (2), pp. 123–132
- [6] Zhang, D., Shi, P., Wang, Q.-G., *et al.*: 'Analysis and synthesis of networked control systems: a survey of recent advances and challenges', *ISA Trans.*, 2017, **66**, pp. 376–392
- [7] Gupta, R.A., Chow, M.-Y.: 'Networked control system: overview and research trends', *IEEE Trans. Ind. Electron.*, 2009, **57**, (7), pp. 2527–2535
- [8] Tabuada, P.: 'Event-triggered real-time scheduling of stabilizing control tasks', *Autom. Control, IEEE Trans.*, 2007, **52**, (9), pp. 1680–1685
- [9] Wang, X., Lemmon, M.D.: 'Event design in event-triggered feedback control systems'. 47th IEEE Conf. Decision and Control, 2008. CDC 2008., Cancun, Mexico, 2008
- [10] Heemels, W., Sandee, J., Van Den Bosch, P.: 'Analysis of event-driven controllers for linear systems', *Int. J. Control*, 2008, **81**, (4), pp. 571–590
- [11] Girard, A.: 'Dynamic triggering mechanisms for event-triggered control', *IEEE Trans. Autom. Control*, 2015, **60**, (7), pp. 1992–1997
- [12] Tripathy, N.S., Kar, I., Paul, K.: 'Stabilization of uncertain discrete-time linear system with limited communication', *IEEE Trans. Autom. Control*, 2016, **62**, (9), pp. 4727–4733
- [13] Yu, H., Hao, F.: 'Input-to-state stability of integral-based event-triggered control for linear plants', *Automatica*, 2017, **85**, pp. 248–255
- [14] Roohi, M.H., Izadi, I., Ghaisari, J.: 'Bandwidth allocation, delay bound analysis, and controller synthesis for event-triggered control systems', *IET Control Theory Appl.*, 2017, **11**, (16), pp. 2870–2878

- [15] Meng, X., Chen, T.: 'Optimal sampling and performance comparison of periodic and event based impulse control', *IEEE Trans. Autom. Control*, 2012, **57**, (12), pp. 3252–3259
- [16] Liu, T., Jiang, Z.-P.: 'Event-based control of nonlinear systems with partial state and output feedback', *Automatica*, 2015, **53**, pp. 10–22
- [17] Wu, Z., Wang, Y., Xiong, J., *et al.*: 'Static output feedback stabilization of networked control systems with a parallel-triggered scheme', *ISA Trans.*, 2019, **85**, pp. 60–70
- [18] Liu, C., Hao, F.: 'Dynamic output-feedback control for linear systems by using event-triggered quantization', *IET Control Theory Applic.*, 2015, **9**, (8), pp. 1254–1263
- [19] Bandyopadhyay, B., Behera, A.K.: '*Event-triggered sliding mode control*' (Springer, Switzerland, 2018)
- [20] Li, H., Shi, Y.: 'Event-triggered robust model predictive control of continuous-time nonlinear systems', *Automatica*, 2014, **50**, (5), pp. 1507–1513
- [21] Wen, S., Yu, X., Zeng, Z., *et al.*: 'Event-triggering load frequency control for multiarea power systems with communication delays', *IEEE Trans. Ind. Electron.*, 2015, **63**, (2), pp. 1308–1317
- [22] Wang, Y.-L., Lim, C.-C., Shi, P.: 'Adaptively adjusted event-triggering mechanism on fault detection for networked control systems', *IEEE Trans. Cybern.*, 2016, **47**, (8), pp. 2299–2311
- [23] Shi, D., Xue, J., Zhao, L., *et al.*: 'Event-triggered active disturbance rejection control of dc torque motors', *IEEE/ASME Trans. Mechatronics*, 2017, **22**, (5), pp. 2277–2287
- [24] Abdelrahim, M., Postoyan, R., Daafouz, J.: 'Event-triggered control of nonlinear singularly perturbed systems based only on the slow dynamics', *Automatica*, 2015, **52**, pp. 15–22
- [25] Bhandari, M., Fulwani, D.M., Gupta, R.: 'Event-triggered composite control of a two time scale system', *IEEE Trans. Circuits Syst. II: Express Briefs*, 2018, **65**, (4), pp. 471–475
- [26] Sivaranjani, K., Rakkiyappan, R., Cao, J., *et al.*: 'Synchronization of nonlinear singularly perturbed complex networks with uncertain inner coupling via event triggered control', *Appl. Math. Comput.*, 2017, **311**, pp. 283–299
- [27] Ma, L., Wang, Z., Cai, C., *et al.*: 'Dynamic event-triggered state estimation for discrete-time singularly perturbed systems with distributed time-delays', *IEEE Trans. Syst. Man Cybern.: Syst.*, 2020, **50**, (9), pp. 3258–3268
- [28] Xu, Q., Zhang, Y., He, W., *et al.*: 'Event-triggered networked H_∞ control of discrete-time nonlinear singular systems', *Appl. Math. Comput.*, 2017, **298**, pp. 368–382
- [29] Song, J., Niu, Y.: 'Dynamic event-triggered sliding mode control: dealing with slow sampling singularly perturbed systems', *IEEE Trans. Circuits Syst. II: Express Briefs*, 2020, **67**, (6), pp. 1079–1083
- [30] Seyboth, G.S., Dimarogonas, D.V., Johansson, K.H.: 'Event-based broadcasting for multi-agent average consensus', *Automatica*, 2013, **49**, (1), pp. 245–252
- [31] Gao, Y.-F., Wang, R., Wen, C., *et al.*: 'Digital event-based control for nonlinear systems without the limit of ISS', *IEEE Trans. Circuits Syst. II: Express Briefs*, 2017, **64**, (7), pp. 807–811
- [32] Ando, Y., Suzuki, M.: 'Control of active suspension systems using the singular perturbation method', *Control Eng. Pract.*, 1996, **4**, (3), pp. 287–293
- [33] Beheshti, M., Nematollahzadeh, S.: 'Design of active suspension control using singular perturbation theory', *IFAC Proc. Vol.*, 2002, **35**, (1), pp. 433–438
- [34] Li, Z., Kolmanovsky, I., Atkins, E., *et al.*: 'Cloud aided semi-active suspension control'. 2014 IEEE Symp. on Computational Intelligence in Vehicles and Transportation Systems (CIVTS), Orlando, FL, USA, 2014
- [35] Zhang, H., Hong, Q., Yan, H., *et al.*: 'Event-based distributed H_∞ filtering networks of 2-dof quarter-car suspension systems', *IEEE Trans. Ind. Inf.*, 2016, **13**, (1), pp. 312–321
- [36] Fei, Z., Wang, X., Liu, M., *et al.*: 'Reliable control for vehicle active suspension systems under event-triggered scheme with frequency range limitation', *IEEE Trans. Syst. Man Cybern.: Syst.*, 2019, doi: 10.1109/TSMC.2019.2899942
- [37] Pan, H., Sun, W., Zhang, J., *et al.*: 'Adaptive event-triggered control for vehicle active suspension systems with state constraints', *IFAC-PapersOnLine*, 2018, **51**, (31), pp. 955–960
- [38] Pan, H., Sun, W., Zhang, J., *et al.*: 'Event-triggered control for active vehicle suspension systems with network-induced delays', *J. Franklin Inst.*, 2019, **356**, (1), pp. 147–172
- [39] Lunze, J., Lehmann, D.: 'A state-feedback approach to event-based control', *Automatica*, 2010, **46**, (1), pp. 211–215
- [40] Behera, A.K., Bandyopadhyay, B.: 'Robust sliding mode control: an event-triggering approach', *IEEE Trans. Circuits Syst. II: Express Briefs*, 2017, **64**, (2), pp. 146–150
- [41] Guinaldo, M., Lehmann, D., Sánchez, J., *et al.*: 'Distributed event-triggered control for non-reliable networks', *J. Franklin Inst.*, 2014, **351**, (12), pp. 5250–5273
- [42] Tallapragada, P., Chopra, N.: 'Decentralized event-triggering for control of LTI systems'. 2013 IEEE Int. Conf. on Control Applications (CCA), Hyderabad, India, 2013
- [43] Guinaldo, M., Sánchez, J., Dormido, R., *et al.*: 'Distributed control for large-scale systems with adaptive event-triggering', *J. Franklin Inst.*, 2016, **353**, (3), pp. 735–756
- [44] Shnayder, V., Hempstead, M., Chen, B.-r., *et al.*: 'Simulating the power consumption of large-scale sensor network applications', Proc. Second Int. Conf. on Embedded Networked Sensor Systems, Baltimore, MD, USA, 2004
- [45] Zhang, H., Zheng, X., Yan, H., *et al.*: 'Codesign of event-triggered and distributed H_∞ filtering for active semi-vehicle suspension systems', *IEEE/ASME Trans. Mechatronics*, 2016, **22**, (2), pp. 1047–1058
- [46] Khalil, H.: '*Nonlinear control*' (Pearson Education Limited, New Delhi zbMATH, 2015, Global edn.)
- [47] 'Active suspension system user manual', Quanser Innovate Educate, 2010